Proceedings of the ASME 2011 Power Conference (POWER 2011)
and the International Conference on Power Engineering 2011 (ICOPE-11)
July 12-14, 2011, Denver, Colorado, USA

POWER2011-55377

EXPERIMENTAL STUDY ON A COMPACT METHANOL-FUELED REFORMER WITH HEAT REGENERATION USING CERAMIC HONEYCOMB (2ND REPORT: REACTION REGION DETECTION BY A POSITIVE ION CURRENT PROBE)

Yasuhiro RAI
Dept. of Mech. Eng. & Sci., Kyoto Univ.
Kyoto, Japan

Hideyuki KOGAME
Dept. of Mech. Eng. & Sci., Kyoto Univ.
Kyoto, Japan

Kazuya TATSUMI
Dept. of Mech. Eng. & Sci., Kyoto Univ.
Kyoto, Japan

Kazuyoshi NAKABE
Dept. of Mech. Eng. & Sci., Kyoto Univ.
Kyoto, Japan

ABSTRACT

A compact tubular-type fuel reformer was fabricated and operated under fuel-rich combustion conditions of methanol, focusing on the partial oxidation reaction (POR). Ceramic honeycomb strainer blocks were inserted in the reactor. In the authors' previous study, Case-1 of only one honeycomb block insertion showed that the reaction region formed in the downstream of the block. This block worked as a reaction stabilizer. The other condition, Case-2, was operated with the secondary honeycomb block inserted in the downstream of the reaction region in addition to the first block. This geometrical structure sandwiched the reaction region between the two blocks, and the thermal energy possessed by the exhaust gas could be regenerated to the reaction region by radiation exchange between these two blocks, which resulted in enhancing the preheating of the premixed gas. By this effect, the methanol-conversion and hydrogen-production in Case-2 were enhanced by about 10% compared to Case-1.

In the present study, the reaction characteristics of the fuel reformer were investigated in detail, by detecting the location of the reaction region. Detailed temperature profiles in the streamwise direction were measured with traversable thermocouples, and positive ion current distributions corresponding to the reaction region were measured with a Langmuir probe. It was confirmed by the both measurements that there exists a reaction region right after the first honeycomb block which accompanies with sharp temperature gradients. The estimated thickness of the reaction region, however, was as wide as several millimeters to a centimeter, which is believed to be a 'mild reaction' stabilized by the first honeycomb block. In Case-2, the high-temperature region became broader compared to Case-1, which indicates that the enhancement of preheating of premixed gas was achieved by the heat regenerated from the secondary honeycomb block.

1. INTRODUCTION

Hydrogen is considered to be one of the most promising fuels in the path of sustainable society. However, in the transition period until the completion of large scale hydrogen distribution system, reforming devices, which convert easy-to-carry hydrocarbon fuels into hydrogen, must be locally installed. In this research, the goal is to establish advanced system for heat and reaction control in small-scale fuel reformers.

By considering the social and technical trends, bio-fuels may be the most promising hydrogen carriers. Also, in the future, low purified fuels may be used as a reformant due to the depletion of energy resources. Such low energy density fuels need more advanced design with heat energy management. When it comes to relatively small-sized compact fuel reformers, this consideration is more important, since heat release to the out of the system will be dominant due to its large surface area to volume ratio [1,2].

Okuyama et al. [3] reported that by applying heat regeneration by porous media which works as a radiant converter, it is possible to stabilize super-fuel-rich flame. This porous radiant converter efficiently converts the enthalpy of exhaust gas penetrating through the porous media and realizes energy regeneration to the upstream region of the reactor.

In the authors' previous study [4], the results of a prototype tubular-typed reformer using heat regeneration by ceramic honeycomb were reported. Methanol was used as fuel. A catalyst was not mounted in order to separate the effects of the catalyst characteristics from the thermal effects.

In this study, one of the objectives is to clarify how the heat regeneration affects the reaction characteristic and reforming efficiency. To analyze reactions in the reformer, an ion current probe was introduced to the fuel reformer. For hydrocarbon fuels, in general, it is well known that combustion reactions always accompany an ion-rich region which corresponds to the flame region [5]. Therefore, measuring ion concentration by an ion current probe helps analyzing the flame structure and the kinetics of combustion [6,7]. Detailed temperature profiles were also measured in the reformer. These measurements clearly revealed the connection between the hydrogen production and the reaction characteristics of the methanol fuel reformer, which enables us to establish some guideline for designing compact fuel reformers.

NOMENCLATURE

D	:	Inner diameter of the reactor,	mm
L	:	Thickness of one honeycomb block,	mm
l	:	Thickness of the rib of the honeycomb,	mm
l_P	:	Pitch of the honeycomb cell,	mm
M	:	Mole flow rate,	mol/s
Q	:	Volume flow rate,	cm^3/s
r	:	Coordinate in radial direction,	mm
T	:	Temperature,	K
W	:	Length of honeycomb block,	mm
x	:	Coordinate in streamwise direction,	mm

Greeks

α	:	Methanol conversion ratio
ξ	:	Production ratio with respect to fuel supply
ϕ	:	Equivalence ratio

Subscripts

air	:	value of supplied air
fuel	:	value of supplied fuel
in	:	value at the center axis of the reactor
ex	:	value at the outer wall of the reactor
H2	:	value of hydrogen

2. EXPERIMENTAL METHOD

2.1 Experimental apparatus

Figure 1 shows the schematic and cross-sectional views of the present compact fuel reformer. This reformer was composed of two parts, i.e., the evaporator and reactor. The evaporator was made of a galvanized steel pipe with inner diameter and length of 28mm and 200mm, respectively. A fuel supply port was located on the surface, on which a fuel injector with electric valve was mounted. A rectangular electric signal with appropriate frequency and duty ratio was input to the injector from a function generator (Yokogawa; WE500, WE7281) to control the fuel flow rate. An air supply port was set at the upstream end of the evaporator. Air supplied to this port was provided from a compressor, and the flow rate was controlled by a rotameter with a needle valve (Kofloc; RK1250). On the

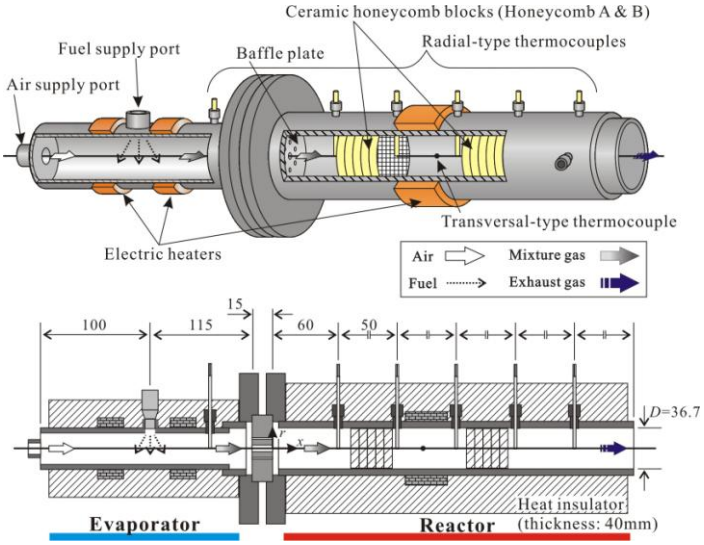

Fig. 1: Experimental apparatus.

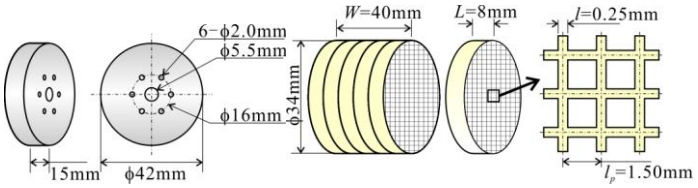

(a) Baffle plate (b) Ceramic honeycomb

Fig. 2: Elements of the reformer.

both side of the fuel supply port, electric band heaters (Sakaguchi E.H Voc Corp.; BH3430) were attached, so that the evaporator could be heated up and held at a specified temperature. Therefore, the fuel injected from the fuel supply port was vaporized instantly after impinging on the high temperature inner wall of the evaporator. The vaporized fuel and air were mixed in the evaporator and then supplied to the reactor through a baffle plate.

As shown in Fig. 1, the baffle plate was located between the evaporator and reactor. Multiple holes were drilled in the 12mm-thick stainless steel disk. The configuration of the holes is shown in Fig. 2 (a). This multi-hole baffle plate was expected to enhance the mixing of fuel and air, and to prevent backfire from the reactor to the evaporator.

The reactor was made of a stainless steel pipe with inner diameter D = 36.7mm and 300mm in length. Several ports were applied on the sidewall of the reactor at the locations shown in Fig. 1. These ports can be used to insert measurement probes and possible multiple reactant supplying nozzles.

Another electric band heater (Hakko; SWD1020) was twined around the reactor at the location of $3.1 \leq x/D \leq 4.3$. This heater was attached for preheating the reactor before the experiment started, so that POR starts smoothly after reactants were supplied.

Ceramic honeycomb blocks shown in Fig. 2 (b) were inserted in several locations in the upstream region of the

reactor, which were expected to enhance heat transfer to the reactant gas and also to utilize heat regeneration from the exhaust gas by using radiative heat transfer. This honeycomb was made of cordierite ceramic, and has mesh of cell number 300. Each block was 8mm thick, so that several blocks were put together by fireproof cement for desired thickness.

Gas sampling for gas component analysis was conducted by inserting a sampling probe into one of the ports on the reactor. The sampling probe was made of stainless steel tube with 3mm in outer diameter. The position of the tip end was set at the reactor centerline, and the gas was collected by connecting the probe outlet to a vacuum-collecting chamber. On the way to the vacuum bottle, a 0.2mm-hole was placed in order to freeze the gaseous reactions. The collected gas was then supplied to a gas chromatograph (Shimadzu; GC-8A) through a filtering chamber packed with silica gel, by which water and unburned methanol were removed from the gas. A gas component detector on the basis of TCD (Thermal Conductivity Detection) method was applied to the gas chromatograph. The column (Shinwa chem.; Shincarbon ST) mounted in the gas chromatograph oven was calibrated for H_2, N_2, O_2, CO, and CO_2. Argon was used as the carrier gas.

2.2 Temperature measurement

Two temperature measurement probes were fabricated: radial-type and transversal-type ones. The radial-type probe was composed of 0.1mm K-type thermocouple wires and two-hole ceramic tube with 3mm in outer diameter. The thermocouple wires were led into each hole and the both ends were welded at the ceramic tube tip. This probe was radially inserted into the reactor at each port located on the reactor side wall so that the gas temperatures at five locations could be measured simultaneously during experiments. The transversal-type probe, on the other hand, was inserted from the uppermost port of the evaporator and stretched along the whole reformer inside with 0.1mm K-type thermocouple wires. By using this type of probe, it was possible to transversally measure gas temperature distributions along with the central axis of the reactor.

The welded junction of thermocouple wires was coated with silica particles by which the probe was prevented from both deteriorating and working as a catalyst for the reaction. Signals from either type of probe were recorded by a personal computer through a digital multi-thermometer (Keyence; NR-1000). The sampling rate and accuracy of the temperature measurement was 10Hz and ±1K, respectively.

2.3 Ion current measurement

It is well known that there exists positive ion in the limited narrow region corresponding to the region where oxidation reaction of hydrocarbon fuel is taking place. There are many studies on the correlation between positive ion distribution and kinetics of flame propagation or turbulent flame by using ion current probe method or mass-spectrometry. Ion current probe method is widely used in combustion analyses due to its simplicity and inexpensiveness. In this study, an ion current probe was fabricated and inserted to the reactor in order to detect the POR of methanol.

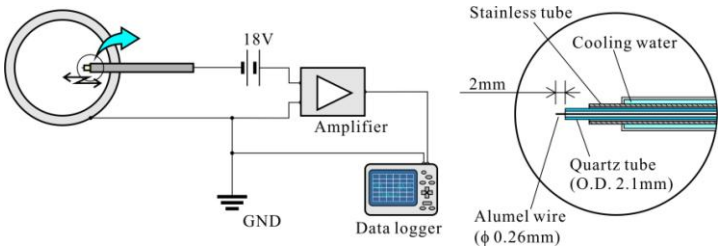

Fig. 3: Langmuir probe and its configuration.

Table 1: Flow rate conditions (Q_{fuel} = 0.092cm^3/s).

ϕ	3.0	3.5	4.0	4.5
Q_{air} [L/min]	7.65	6.56	5.74	5.10

Figure 3 shows the ion current probe, so-called Langmuir probe, and its configuration including amplifying circuit. A 0.26mm-in-diameter alumel wire was used as an ion current sensor and extended for 2mm in length from the tip of quartz glass tube (O.D. 2.1mm). The quartz glass tube was surrounded with a stainless tube with water cooling system, so that the probe was not excessively heated which causes thermal noise. Negative electric potential, -18V, relative to the grounded reactor wall was imposed on the ion current probe. Positive ion current flowing into the probe was observed through an amplifier with a current-voltage converter (Hamamatsu; C7319). The gain of the amplifier was 10^6 V/A. Amplified voltage signal was obtained by an A/D converter (Keyence; NR-1000) with sampling rate 10Hz and analyzed by PC.

3. EXPERIMENTAL CONDITIONS

In this study, we investigate how the ceramic honeycomb blocks affect reforming characteristics and reaction efficiencies. First as Case-1, one honeycomb block (called Honeycomb A) with thickness of 40mm was inserted in the region of the reactor, $1.8 < x/D < 2.9$. Case-1 is the experiment where basic reformer characteristics were investigated without using positive heat regeneration; Honeycomb A was inserted to maintain a stable reaction under fuel-rich operation conditions by increasing the heat transfer to the reactant gas. If honeycomb block was not inserted at all in the reactor, POR did not occur for any fuel-rich equivalence ratio conditions.

Second as Case-2, another honeycomb block with the same thickness (called Honeycomb B) was inserted downstream of Honeycomb A. Honeycomb B was expected to play the role of positive heat regeneration, i.e., the enthalpy of exhaust gas was absorbed by Honeycomb B when the gas flow through it, and a portion of the enthalpy was regenerated to the upstream reaction region by radiative and conductive heat transfer. By using energy regeneration from the exhaust gas, the reforming efficiency could be increased. Honeycomb B was inserted downstream of Honeycomb A with streamwise space of 1.6*D*, which works as a reaction region of POR. It was confirmed that

enough space for reaction was needed to stabilize POR in this reformer. This is because the reaction speed of POR is considerably slower than the complete combustion reaction due to fuel-rich POR conditions.

As described in the previous section, experiments were carried out with regard to POR of methanol. Table 1 shows the flow rate conditions of reactants. Fuel and air were both supplied to the reactor from the evaporator through the baffle plate. Q_{air} and Q_{fuel} are the volume flow rates of the air and fuel fed to the evaporator, respectively. Note that Q_{fuel} represents the volume flow rate of the fuel in liquid form. ϕ is the equivalence ratio based on the complete combustion reaction. The stoichiometric equivalence ratio of the POR, therefore, is $\phi = 3$. As shown in Table 1, Q_{fuel} was fixed to one value in the present experiments, and Q_{air} was varied in the range of equivalence ratios, $3.0 \le \phi \le 4.5$.

The procedure applied in the reaction experiment is described as follows. The evaporator and reactor pipes were first heated by the electric band heaters so that the temperatures measured at the locations of $x/D = -3.9$, upstream of the baffle plate rear surface, and $x/D = 3.0$ reached 470K and 820K, respectively. Then, the heaters attached to the reactor were turned off and the fuel and air were supplied to the reformer. Note that the heaters of the evaporator continued to be powered during the experiment and the temperature inside the evaporator was kept at about 420K.

4. RESULTS AND DISCUSSION

4.1 Parameters for performance evaluation

In the present study, the quantity of the consumed methanol cannot be measured directly due to the absorption of water and unreacted methanol in the silica gel chamber. Therefore, these quantities were estimated from the concentrations of the other gases included in the exhaust gas. Since the summation of the analyzed concentrations of H_2, N_2, O_2, CO, and CO_2 in the exhaust gas was 100±2%, the major components of the gas was expected to be these five species plus water and unreacted methanol that were collected in the silica gel chamber. When paying attention to carbon atoms, the components possessing carbon atoms among the products are CO, CO_2 and unreacted methanol. Thus, the quantity of the consumed methanol can be calculated using the concentrations of CO and CO_2 in the exhaust gas. The methanol conversion ratio, α, is defined as follows:

$$\alpha \equiv \frac{M_{\mathrm{CH3OH,consumed}}}{M_{\mathrm{CH3OH,supplied}}} = \frac{M_{\mathrm{CO}} + M_{\mathrm{CO2}}}{M_{\mathrm{CH3OH,supplied}}} = \frac{Y_{\mathrm{CO}} + Y_{\mathrm{CO2}}}{Y_{\mathrm{N2}}} \times \frac{M_{\mathrm{N2}}}{M_{\mathrm{CH3OH,supplied}}} \quad (1)$$

where M_X is the molar flow rate of the X component in the exhaust gas, and Y_X is the X's concentration.

To evaluate the production efficiency of each component, the production rate of component X against 1mol of methanol supplied, ξ_X, is defined as follows:

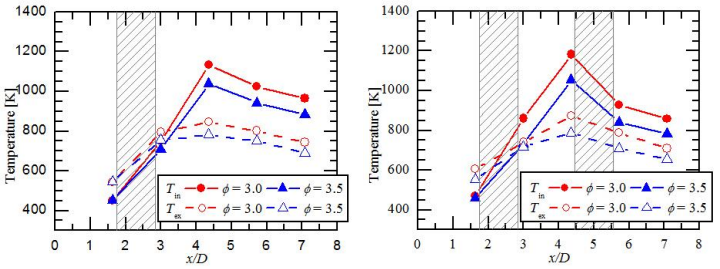

(a) Case-1 (b) Case-2

Fig. 4: Temperature distributions (measured by radial-type probes).

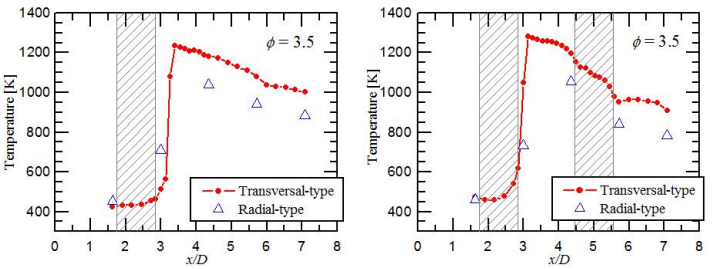

(a) Case-1 (b) Case-2

Fig. 5: Temperature distributions (measured by two types of probes, $\phi = 3.5$).

$$\xi_X \equiv \frac{M_X}{M_{\mathrm{CH3OH,supplied}}} = \frac{(Y_X / Y_{\mathrm{N2}}) M_{\mathrm{N2}}}{M_{\mathrm{CH3OH,supplied}}} \quad (2)$$

4.2 Temperature profiles

The present fuel reformer was possible to operate under as wide conditions as of equivalence ratio, ϕ, between 3.0 and 4.5. Figure 4 shows the streamwise temperature distributions measured by the redial-type probes for the cases $\phi = 3.0$ and 3.5 in Case-1 and -2. The ordinate indicates the temperature measured, and the abscissa indicates the dimensionless streamwise coordinate x/D from the downstream surface of the baffle plate. Hatched region in the graph corresponds to the location of Honeycomb A or B.

For Case-1, temperature distributions show similar trend regardless of ϕ condition. Distributions of gas temperature on the centerline of the reactor, T_{in}, plotted by solid symbols and lines, take their maximum values at $x/D = 4.4$ and the temperature decreases downstream. It is inferred from these temperature distributions that the main exothermic reaction took place in the region of $3.0 \le x/D \le 4.4$. In $x/D \ge 4.4$, the temperature decreases as x/D increases, which shows that an exothermic reaction did not take place in the downstream region. The surface temperature of the reactor side wall, T_{ex}, which is plotted by open symbols and broken lines, does not experience a sudden temperature increase as seen in T_{in} but corresponds moderately to T_{in}. The most upstream surface temperature, T_{ex}, monitored at $x/D = 1.6$, was slightly higher than the corresponding gas temperature, T_{in}, which was caused by heat conduction through the side wall from the downstream

of the reactor. However, T_{ex} shows its maximum value at x/D = 4.4 which is the same trend as T_{in}.

Comparing the temperature distributions in Fig. 4 with regard to equivalence ratio, ϕ, temperature level decreases as ϕ increases. This is due to the fact that when ϕ becomes small, the oxygen supply rate to methanol increases, which results in promoting the exothermic oxidative reaction and increasing the temperature of the reforming gas.

Figure 4 (b) shows the temperature distributions of Case-2, which is the case with heat regeneration by the second honeycomb block applied. By comparison with Case-1, temperature rise between Honeycombs A and B ($3.0 \leq x/D \leq 4.4$) and temperature drop downstream of Honeycomb B ($x/D \geq 5.7$) were observed for both ϕ conditions.

Figure 5 shows the temperature profiles of ϕ = 3.5 for Case-1 and -2 measured by both transversal-type and radial-type probes. By using the former probes, temperature information between the latter probes could be obtained. The values of temperature disagree between the former (solid symbol and line) and the latter (open symbol) at high temperature region; higher temperature values were obtained by the former. The differences between these values are about 100K, which is believed to be caused by radiative effect.

As described before, the latter probe was composed of 3mm ceramic tube (with two holes), and thermocouple wires were welded together at the tip of the tube. Since the temperature sensing junction of thermocouple has contact with the ceramic tube tip, the temperature value obtained is affected by temperatures of both surrounded gas and ceramic tube solid. Ceramic solid surface has larger property of emissivity compare to the other metallic materials, so irradiation from the ceramic surface together with the radial conduction cools down the ceramic tube itself, which causes the temperature value by the latter radial-type probe to be lower than that by the former transversal-type probe. For the transversal-type probe, on the contrary, a higher temperature can be monitored due to the axial conduction through the thermocouple wire from both the higher temperature downstream region and the lower temperature upstream region. In spite of these thermal effects, these temperature values themselves can still be used for qualitative discussion.

In Fig. 5 (a), temperature takes almost constant value 470K within Honeycomb A, and very steep temperature gradient exists in the downstream region. This sudden temperature increase corresponds to the region where exothermic oxidative reaction takes place. The maximum temperature value 1230K was observed at x/D = 3.4 which is 20mm downstream from the outlet of Honeycomb A. In the post-reaction region x/D > 3.4, temperature decreases downstream. From this temperature profile, POR begins in the downstream of Honeycomb A.

Figure 5 (b) depicts temperature profiles of Case-2. Temperature within Honeycomb A shows different characteristics from Case-1, i.e., temperature rise begins from the inside of Honeycomb A. The temperature at the outlet of

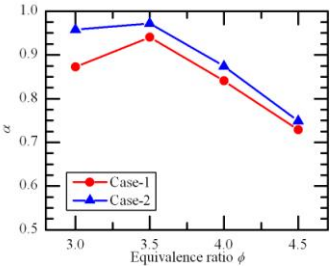

Fig. 6: Methanol conversion ratio, α, (Cases-1&2).

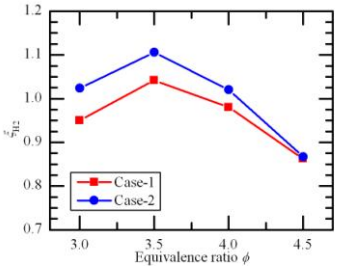

Fig. 7: Hydrogen production ratio, ξ_{H2} (Cases-1&2).

Honeycomb A was about 670K, which is 200K higher than Case-1. While the maximum temperature was observed at x/D = 3.1 for Case-2, which is about 10mm upstream-side of Case-1. From these results, the reaction of Case-2 starts from more upstream region than Case-1, since Honeycomb B worked as an energy regenerator and increased the temperature of Honeycomb A by radiative energy exchange.

A large temperature decrease within Honeycomb B was observed in Case-2. This temperature drop was caused by absorption of the exhaust gas enthalpy by Honeycomb B. The temperature difference between the inlet and outlet of Honeycomb B is about 180K, monitored by either probe. This temperature drop proves that Honeycomb B absorbs a portion of enthalpy possessed by the exhaust gas and works as an energy regenerator.

4.3 Reforming efficiency

Figure 6 shows the relation between methanol conversion ratio, α, and ϕ. For both Case-1 and -2, α takes its maximum value at ϕ = 3.5 and decreases as ϕ increases. Much larger equivalence ratio represents excessive fuel-rich condition, which means the lack of oxygen supply and causes smaller methanol conversion ratio compared to the smaller ϕ conditions. For all ϕ conditions, Case-2 has larger α values compared to Case-1. This is because energy regeneration caused by Honeycomb B increased the temperature between Honeycombs A and B, which resulted in higher decomposition ratio of methanol.

The hydrogen production ratio, ξ_{H2}, is shown in Fig. 7. ξ_{H2} takes its maximum value at ϕ = 3.5, and decreases in the region of ϕ > 3.5. This trend is similar to the methanol conversion ratio, α. This result indicates that the production efficiency of hydrogen is greatly affected by the methanol conversion ratio. Thus, if it is possible to increase α close more to unity, it may result in larger hydrogen production. However, α is already more than 96%. Other effective reaction paths from methanol to hydrogen should be searched for the improvement of hydrogen production efficiency.

4.4 Positive ion detection

From the results of temperature distributions discussed in Section 4.2, the reaction region was formed at the outlet of Honeycomb A. Positive ion current detection by ion current

probe was conducted to precisely ensure the location of the reaction region.

Ion current was observed only at x/D = 3.0. At post-reaction region like x/D = 4.4, soot deposition disturbed the ion current detection. Operated under fuel-rich conditions, the cooled ion current probe promoted soot formation on the surface of the ion current probe in the post-reaction region which caused break-down of the electrical insulation of the probe.

Figure 8 shows the radial distributions of ion current for both Case-1 and -2 at x/D = 3.0, which is 6mm downstream of the outlet of Honeycomb A. For Case-1, regardless of ϕ conditions, ion current was within almost negligible level. This indicates that reactions involving positive ions were still not activated at x/D = 3.0. Although Fig. 5 (a) indicates that there exists large temperature gradient at x/D = 3.0, ion current was not detected here, which means that this region is so-called pre-heat region, where thermal pyrolysis reactions are taking place.

However, for Case-2 at the same x/D location, large ion current was observed for both ϕ = 3.0 and 3.5. This is due to the fact that heat regeneration from Honeycomb B made reaction region moving upstream. In this case, pre-heat region moves inside Honeycomb A, which enhances the pyrolysis reaction since thermal energy for pyrolysis is supplied not only from the reaction region by thermal conduction through the reactant gas but also from Honeycomb B by means of radiative energy exchange.

Comparing Fig. 8 (a) and (b), ϕ =3.5 experiences higher ion current for Case-2. The result implies that the combustion reaction region can be shifted a bit upstream or the active formation of soot might be detected here. Calcote et al. [8] reported that the minimum ion concentration of hydrocarbon fuel is reached in a slightly sooting flame. Larger ϕ cases with further fuel enrichment have the possibility of the growth of ion current related to soot formation which involves much large molecules.

5. CONCLUSIONS

In the present article, major conclusions obtained are listed in the following:

- A methanol fuel reformer was fabricated and operated under the conditions of $3.0 \leq \phi \leq 4.5$. A better performance was obtained under the conditions of ϕ = 3.5.
- Temperature distribution measured by the transversal-type probe showed about 100K higher than that by radial-type one.
- For the single honeycomb insertion (Case-1), POR begins about 10mm downstream of Honeycomb A, while ion current was not observed at x/D = 3.0 which was located in the pre-heat region of the reaction.
- At the outlet of Honeycomb A for the double honeycomb insertion (Case-2), much higher temperature (200K higher) was observed than for Case-1.
- Reaction in Case-2 began about 10mm upstream compared to Case-1 and ion current was detected at x/D = 3.0, which is caused by the energy regeneration effect by the downstream honeycomb block.
- By increasing the equivalence ratio from ϕ = 3.0 to 3.5, ion current level was increased possibly because of the upstream shift of the reactions or active formation of soot.

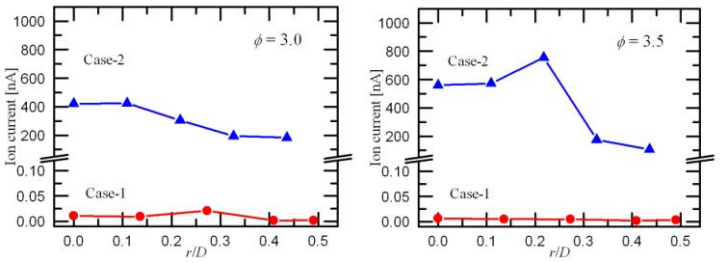

(a) ϕ = 3.0 (b) ϕ = 3.5

Fig. 8: Radial distributions of ion current at x/D = 3.0.

ACKNOWLEDGMENTS

The authors express their thanks to Kyocera Corporation, Toyota Central R&D Labs., Inc., and Mitsubishi Electric Corporation for the supply of some experimental device parts.

REFERENCES

[1] B. Li, S. Kado and Y. Mukainakano, "Temperature Profile of Catalyst Bed during Oxidative Steam Reforming of Methane over Pt-Ni Bimetallic Catalysts", *Applied Catalysis A General*, 304 (2006), pp. 62-71.

[2] C. Pan, R. He and Q. Li, "Integration of High Temperature PEM Fuel Cells with a Methanol Reformer", *J. Power Sources*, 145 (2005), pp. 392-398.

[3] M. Okuyama, K. Hanamura, R. Echigo and H. Yoshida, "Flame Structure of Super Fuel-Rich Premixed Flame", *Transactions of the Japan Society of Mechanical Engineers (Ser. B)*, 61 (1995), pp.2724-2730 (in Japanese).

[4] Y. Rai, K. Tatsumi and K. Nakabe, "Experimental Study on a Compact Methanol-Fueled Reformer with Heat Regeneration Using Ceramic Honeycomb", *Proc. Int'l Heat Transfer Conference 14*, (2010), IHTC14-22742.

[5] J. M. Goodings, D. K. Bohme and T. M. Sugden, "Positive Ion Probe of Methane-Oxygen Combustion", *Proc. 16th Symp. (Int'l) on Combustion*, 16 (1977), pp.891-902.

[6] H. Naito and A. Yoshida, "Ion Current Characteristics in a Stirred Reactor", *Transactions of the Japan Society of Mechanical Engineers (Ser. B)*, 68 (2002), pp.256-259 (in Japanese).

[7] P. Mehresh, J. Souder, D. Flowers, U. Riedel and R. W. Dibble, "Combustion Timing in HCCI Engines Determined by Ion-sensor: Experimental and Kinetic Modeling", *Proc. Combustion Institute*, 30 (2005), pp.2701-2709.

[8] H. F. Calcote, D. B. Olson and D. G. Keil, "Are Ions Important in Soot Formation?", *Energy and Fuels*, 2 (1988), pp.494-504.